Ferroelectrics, 1991, Vol. 113, pp. 305–322
Reprints available directly from the publisher
Photocopying permitted by license only

INFLUENCE OF ZIG-ZAG DEFECTS ON ELECTROMECHANICAL RESPONSES OF PLANAR S_C^* LIQUID CRYSTALS

ANTAL JÁKLI, NÁNDOR ÉBER and LAJOS BATA
Central Research Institute for Physics,
H-1525 Budapest, P.O.Box 49, Hungary

Abstract The resonances found in the frequency spectra of the electromechanical responses of various planar S_C^* liquid crystal samples are explained theoretically. The theory supplements the continuum theory of uniform S_C^* liquid crystals by taking into account the influence of zig-zag defects, which are between the oppositely bent domains. The influence of focal-conic defects present in non perfectly aligned textures is discussed too.

INTRODUCTION

In the last some years planar S_C^* liquid crystals have been investigated very intensively.

Due to their special symmetry properties they are ferroelectric and also piezoelectric. Ferroelectricity (the presence of spontaneous polarization) results in strong interaction between the director and the external electric field, consequently it promises fast electrooptical responses[1]. The electrooptical investigations helped not only to invent practically applicable devices, but, in addition clarified the picture about the sample structure. On the basis of these studies it has turned out, that the smectic layers are bent, producing the so called "chevron" structure[2,3].

Piezoelectricity results in interesting electromechanical[4-7], and mechano-electrical[8,9] effects. As it was

pointed out[4], applying alternating electric fields onto planar aligned S_C^* liquid crystal samples mechanical vibrations appear in the direction perpendicular to both the electric field and the smectic layer normal. The inverse of this electromechanical effect (the mechano-electrical effect) means that an external shear of a sandwich cell induces electrical charges on the electrodes of the bounding substrates.

Experiments have proved the presence of several resonances in the frequency spectra of the above phenomena.[6,7,9] In cases of homogeneous alignment the frequencies of the observed resonances f_1 and f_2 were independent of the mass of the moving plate, while if focal-conic defects were present an additional resonance appeared at a frequency f_o which was shifted with the mass.[6] In samples of both type zig-zag defects were observed under the microscope.

The resonance frequencies were found to be in the kHz range and decreased slightly as the S_A - S_C^* phase transition temperature was approached.

Comparing the resonances found in the spectra of linear and quadratic electromechanical as well as the mechano-electrical responses it was suggested[6] that the resonances may be related to the chevron structure of planar S_C^* samples.

In this paper we present a theoretical model which supports this relation. We point out that the resonances at f_1 and f_2 frequencies are due to the elastic behaviour of the zig-zag defects, while the one at f_o is the result of focal-conic defects.

MODEL

Geometry of planar S_C^* liquid crystal samples.

The latest investigations on planar S_C^* samples pointed out that both in thick and in thin samples the smectic layers are not simply planes standing perpendicularly to the bounding plates, but are bent[2,3]. The creation of bent

layers can be explained as follows[10]. At the S_A - S_C^* phase transition temperature the smectic layer thickness decreases due to the director tilting (θ) from the layer normal ($\underline{n}$). To keep the density constant, either the number of layers or the area of each layer must be increased. Since the Nambu-Goldstone mode[10] of smectic layer undulation is easily excited at the phase transition a bend occurs in order to increase the smectic layer area. The most favourable bent structures are the chevrons. Two kinds of oppositely bent layers (<<< and >>>) may be present in planar samples. These form domains which are separated from each other by the so called zig-zag defects (<<<*>>> type forms the so called "lightning", while >>>*<<< type yields the "hairpin" defects.)

According to the model worked out by Clark et al[11] a planar sample is schematically illustrated in Figure 1. Though the details have not yet been clarified, we can say that the "zig-zag" defects are composed of straight parts running parallel to the smectic layers, and of zig-zag parts which are nearly perpendicular to those.

As the mechanical vibration is parallel to the layers of the monodomains, the effect of straight defect lines is negligable. Nevertheless the zig-zag parts (presented in Fig.2) will respond elastically to mechanical vibrations.

The force induced on the unit length of a zig-zag defect can be calculated as follows.

Let us denote the displacements of a monodomain <<< and >>> by $\underline{s}^+(x)$ and $\underline{s}^-(x)$ respectively. During vibration the defect line separating the two domains becomes deformed if the difference of displacements

$$\Delta\underline{s}(x) = \underline{s}^+(x) - \underline{s}^-(x) \qquad (1)$$

does not equal to zero. Following the notation of Ref.(11) and analyzing Fig.(2) we can obtain for the variation of a smectic layer thickness (Δd) that in case of small displacements

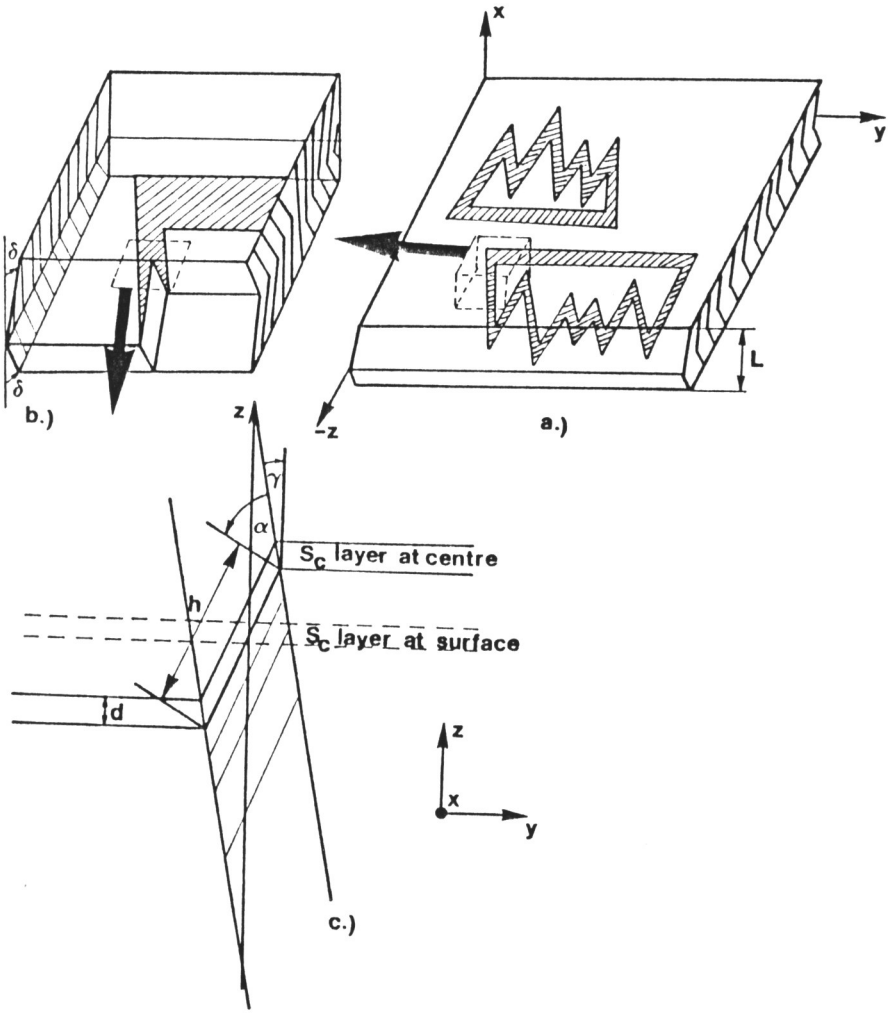

FIGURE 1. Schematic representation of the chevron structure of planar S_C^* liquid crystal samples.

a.) Typically $1cm^2$ area sample with three domains.
b.) Typically $1mm^2$ area sample representing one zig-zag defect between oppositely bent domains.
c.) Typically $30\mu m \times 30\mu m$ area representing the structure of one zig-zag line.

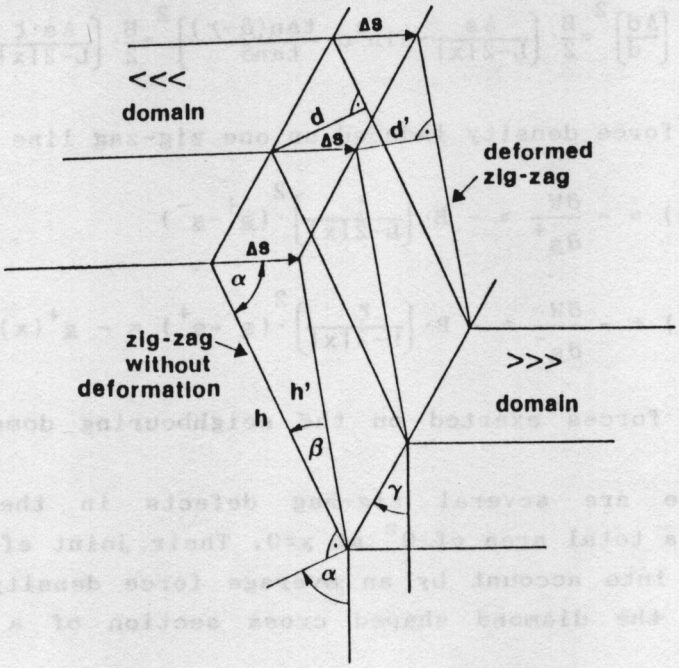

FIGURE 2. Deformation of one zig-zag line due to the electromechanical vibration in the centre of the sample. The difference of displacements of the two oppositely bent monodomains is Δs.

$$\frac{\Delta d}{d} \approx \frac{\Delta s(x)}{h(x)} \cdot \tan(\alpha-\gamma)\sin\alpha \qquad (\Delta s \ll h). \qquad (2)$$

In this expression d is the smectic layer thickness, h(x) the width of the defect line and the meaning of angles α and γ are seen in Figs.1c and 2. The leaning angle δ of the bent layers is generally[11] $\delta \leq \theta$ (θ is the tilt angle of the director). According to observations the above relation is independent of temperature, furthermore $\gamma < 20\text{-}30^\circ$ and $\alpha \approx \gamma$. Taking into account the diamond shaped cross-section of the defect line simple geometrical considerations yield

$$h(x) = \left[L-2|x|\right] \cdot \frac{\tan\delta}{\sin\alpha} \qquad (3)$$

where L denotes the thickness of the sample.

The contribution of the smectic layer compression into

the free energy density W reads

$$W=\frac{B}{2}\cdot\left[\frac{\Delta d}{d}\right]^2=\frac{B}{2}\cdot\left[\frac{\Delta s}{L-2|x|}\cdot\sin^2\alpha\cdot\frac{\tan(\delta-\gamma)}{\tan\delta}\right]^2=\frac{B}{2}\cdot\left[\frac{\Delta s\cdot\xi}{L-2|x|}\right]^2. \quad (4)$$

Then the force density induced on one zig-zag line reads

$$\begin{aligned} \underline{g}^+(x) &= -\frac{\partial W}{\partial \underline{s}^+} = -B\cdot\left[\frac{\xi}{L-2|x|}\right]^2\cdot(\underline{s}^+-\underline{s}^-) \\ \underline{g}^-(x) &= -\frac{\partial W}{\partial \underline{s}^-} = -B\cdot\left[\frac{\xi}{L-2|x|}\right]^2\cdot(\underline{s}^--\underline{s}^+) = -\underline{g}^+(x) \end{aligned} \quad (5)$$

i.e. the forces exerted on the neighbouring domains are opposite.

There are several zig-zag defects in the sample covering a total area of Ω^z at x=0. Their joint effect can be taken into account by an average force density $\underline{f}^{\pm}(x)$. Owing to the diamond shaped cross section of a zig-zag defect

$$\underline{f}^{\pm}(x) = g^{\pm}(x)\cdot\frac{\Omega^z}{\Omega}\cdot\left[1-\frac{2|x|}{L}\right] = -\pm c(x)\cdot(\underline{s}^+-\underline{s}^-) \quad (6)$$

where Ω is the total sample area.

This expression indicates an elastic force with the effective "spring constant" c(x). The form of c(x) follows from Eqs.(5) and (6)

$$c(x) = \dot{c}\cdot\left[1-\frac{2|x|}{L}\right]^{-1}. \quad (6a)$$

Let us estimate the magnitude of $\dot{c}$. From microscopical observations[6] we know that the average dimensions of monodomains are very different in various materials, e.g. in FK4 $\Omega^d\approx10^{-4}m^2$ while in CS1011 $\Omega^d\approx10^{-6}m^2$. Taking into account that generally the diameter of a zig-zag defect is in the order of sample thickness ($\approx10^{-5}$m) we can estimate $\Omega^z/\Omega\approx10^{-2}$-$10^{-3}$. Taking $B\approx10^6Nm^{-2}$, and using typical values[11] for the other parameters present in the expression of $\dot{c}$, we obtain $\dot{c}\approx10^{10}$- $10^{11}Nm^{-4}$.

Equation of motion of substances

We regard the material as an incompressible and electrically insulating continuum and we use the description worked out for monodomains in Ref.(12). Though a real sample is a complicated composition of <<< and >>> domains and the separating zig-zag defects, in our model we have to limit ourselves to monodomains whose interaction will be taken into account by the volume force introduced above and the boundary conditions being discussed later on. Thus the modified balance equation of the linear momentum reads

$$\rho \frac{d^2 s_i^{\pm}}{dt^2} = - \nabla_j \sigma_{ij}^{\pm} + f_i^{\pm} \ . \tag{7}$$

Here $\sigma_{ij}^{\pm}$ is the i,j-th component of the mechanical stress tensor of the medium, $f_i^{\pm}$ the i-th component of the force density originating in defects, ρ the substance density, ∇_j the space derivative with respect to the j-th coordinate and the upper indices (±) refer to the type of the domains.

We can suppose that the monodomains are homogeneous in the yz plane and we investigate only displacements in the y direction . Then $\underline{s}^{\pm}=(0,\ s^{\pm}(x),\ 0)$ and only σ_{yx} enters into Eq.(7).

Following the notation of Ref.(12)

$$\sigma_{yx}^{\pm} = L_{yxyx}^{66\pm} \nabla_x \left(\frac{ds_y^{\pm}}{dt} \right) + L_{yxx}^{65\pm} \frac{dE_x}{dt} \tag{8}$$

is obtained where $L_{yxyx}^{66\pm}$ and $L_{yxx}^{65\pm}$ are the Onsager coefficients corresponding viscosity and electromechanical coupling respectively.

Considering the sample geometry presented in Figs.1 and 3a the vectors of electric field $\underline{E}$, smectic layer normal $\underline{n}$, and C-director $\underline{c}$ can be expressed as

$$\underline{E}^{\pm} = (E,\ 0,\ 0) \quad ; \quad \underline{n}^{\pm} = (\pm \mathrm{sgn}x \cdot \sin\delta,\ 0,\ \cos\delta)$$

$$\underline{c}^{\pm} = (\sin\varphi \cdot \cos\delta,\ \cos\varphi,\ -\pm \mathrm{sgn}x \cdot \sin\delta \cdot \sin\varphi), \tag{9}$$

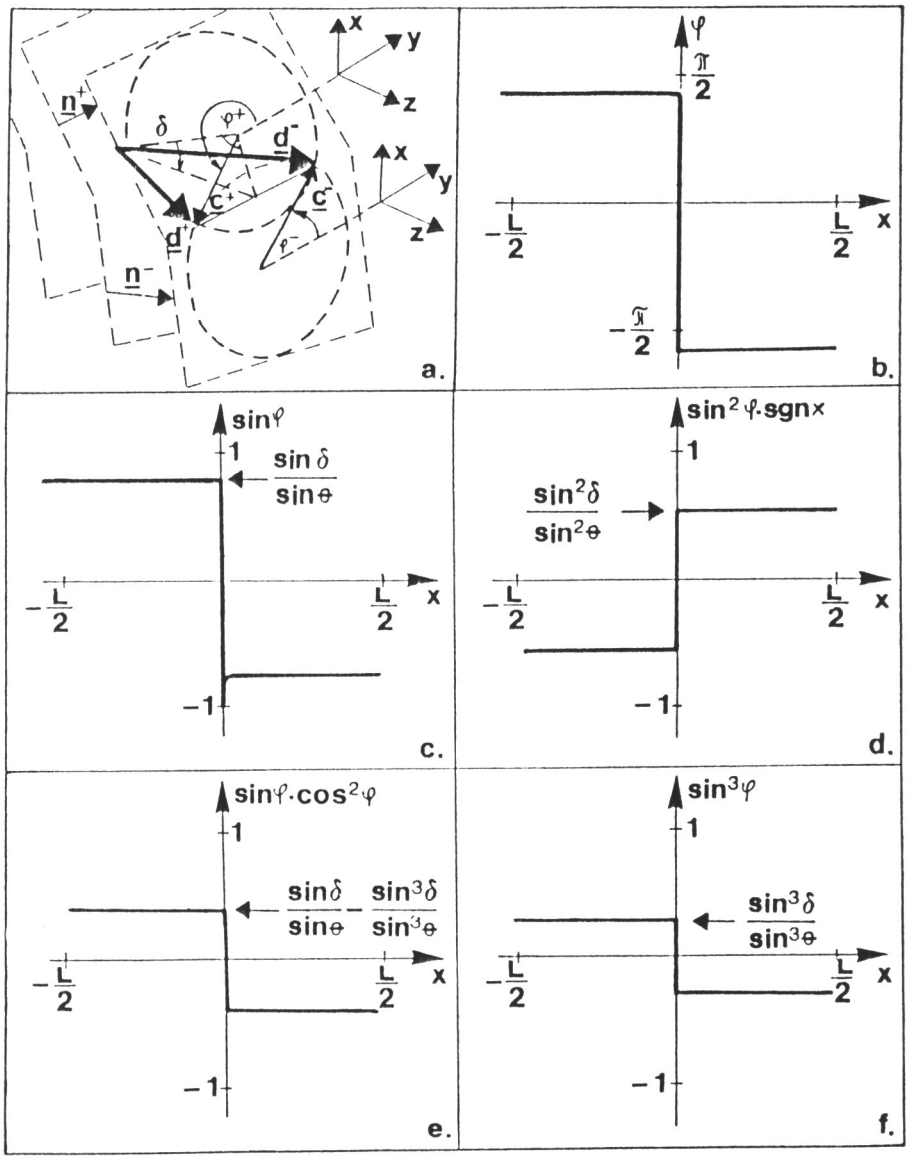

FIGURE 3. The geometry of a surface stabilized sample and the x dependences of the azimuthal angle φ, and its various functions.

where $\mathrm{sgn}x = \begin{cases} 1 & \text{if } x>0 \\ -1 & \text{if } x<0 \end{cases}$.

Using Eqs.(3.23) and (3.22) of Ref.(12) we obtain from Eq.(9) that

$$L^{66\pm}_{yxyx} = \cos^2\delta\sin^2\varphi\cdot(\mu_5\cos^2\varphi+\mu_{11}) + \sin^2\delta\cdot(\mu_8\cos^2\varphi+\mu_{12}) + \mu_{11}\cos^2\varphi + \pm\mathrm{sgn}x\sin2\delta\sin\varphi\cdot(\mu_9\cos^2\varphi+\mu_{13}) \quad (10)$$

$$L^{65\pm}_{yxx} = -\cos^2\delta\sin\varphi\cdot(\gamma_2\cos^2\varphi+\gamma_5\cos2\varphi) + \gamma_8\sin^2\delta\sin\varphi - \pm\mathrm{sgn}x\sin\delta\cos\delta\cdot(\gamma_4\cos^2\varphi+\gamma_6\cos2\varphi-\gamma_7\sin^2\varphi). \quad (11)$$

In a typical chevron structure the azimuthal angle φ of the C-directors on the bounding plates differ from each other by π. Furthermore the same difference can be found on the same surface but in different domains.

	<<< domain	>>> domain
$x = \frac{L}{2}$	$\varphi = \varphi_0$	$\varphi = \varphi_0 + \pi$
$x = -\frac{L}{2}$	$\varphi = \varphi_0 + \pi$	$\varphi = \varphi_0$

Going along the x direction this rotation of the C-director takes place at the centre of the sample (x=0) within a very short distance 2λ ($\lambda \leq 0.01\mu m$)[11] which can be neglected with respect to other characteristic distances. Thus either $\varphi=\varphi_0$ or $\varphi=\varphi_0+\pi$ with $\sin\varphi_0=\frac{\sin\delta}{\sin\theta}$ holds for the whole sample except in the centre. As shown in Fig.3 all functions of φ appearing in Eq.(11) can be approximated by the function H(x)

$$H(x) = \begin{cases} -1 & \text{if } x < -\lambda \\ 1 & \text{if } x > \lambda \end{cases} \qquad (\lambda \longrightarrow 0).$$

Thus instead of Eqs.(10) and (11) we can use the formulae

$$L^{66\pm}_{yxyx} \approx \mu \quad \text{and} \quad L^{65\pm}_{yxx} \approx -\pm\gamma\cdot H(x). \quad (12)$$

With these relations the equation of motion of the substance Eq.(2) can be rewritten as

$$\rho\cdot\frac{d^2s^{\pm}}{dt^2}=-\mu\cdot\nabla_x^2\left(\frac{ds^{\pm}}{dt}\right)+\pm\gamma\cdot\frac{dE}{dt}\cdot\nabla_x H(x)-\pm\frac{\dot{c}}{1-\frac{2|x|}{L}}\cdot(s^+-s^-). \qquad (13)$$

We are interested in the linear electromechanical response to a harmonic electric field $E(t)=E\cdot e^{i\omega t}$, so Eq.(13) can be transformed into the set of equations

$$\omega^2\rho\cdot(s^++s^-)=i\omega\mu\cdot\nabla_x^2(s^++s^-)$$

$$\omega^2\rho\cdot(s^+-s^-)=i\omega\mu\cdot\nabla_x^2(s^+-s^-)-2i\omega\gamma E\cdot\delta(x)+\frac{2\dot{c}}{1-\frac{2|x|}{L}}\cdot(s^+-s^-) \qquad (14)$$

where

$$\delta(x)=\nabla_x H(x)=\begin{cases}\frac{1}{\lambda} & \text{if } |x|<\lambda\\ 0 & \text{if } |x|>\lambda\end{cases} \qquad \lambda\longrightarrow 0.$$

These formulae show that the electric field interacts with the substance only in a very thin region in the middle of the sample, where the smectic layer bend and the director rotation takes place. Furthermore the electric field is coupled to s^+-s^- only while the response of s^++s^- is purely viscous.

We have to mention that in the strict sense of word the treatment outlined above is applicable only for surface stabilized ferroelectric samples since we neglected the z dependence of various quantities and this does not hold in the presence of a helix. However, if we are not interested in phenomena taking place on the length scale smaller than the pitch an averaging over the pitch can be done (coarse grained description). It is expected that in this limit we should obtain similar equations but with different, averaged material parameters (e.g. $\langle\mu\rangle$ and $\langle\gamma\rangle$ instead of μ and γ in Eq.(12)). This suggests that our results are applicable for thick samples as well.

Boundary conditions

To solve Eq.(14) we also need to consider the boundary conditions.

The bottom plate $\left(x=-\frac{L}{2}\right)$ is fixed, thus $s^{+}\left(-\frac{L}{2}\right)=0$ and $s^{-}\left(-\frac{L}{2}\right)=0$. The top plate $\left(x=\frac{L}{2}\right)$ performs an oscillation forced by the vibration of the liquid crystal. The displacement of the top plate is described by the vector $\underline{u}=(0, u, 0)$. Since the top plate is common for domains of both type

$$u = s^{+}\left(+\frac{L}{2}\right) = s^{-}\left(+\frac{L}{2}\right) . \tag{15}$$

The displacement u is governed by the equation of motion

$$m \frac{d^2u}{dt^2} = F_y^{\Omega} , \tag{16}$$

where m is the mass of the plate, and F_y^{Ω} the force exerted on the plate by the liquid crystal. This force is a surface force

$$F_y^{\Omega} = \int_{\Omega} \sigma_{yx} d\Omega_x . \tag{16a}$$

Here $d\Omega_x$ is the surface element pointing outward from the sample, and the integration should be carried out over the whole surface Ω of the upper plate.

It is very important to note that, as the cross section of zig-zag defects is diamond shaped, at the boundaries all the smectic layers are parallel to the vibration. Consequently $\Omega=\Omega^{+}+\Omega^{-}$, where Ω^{+} and Ω^{-} are the total surface of <<< and >>> domains respectively. Then Eq.(16) can be transformed into the form

$$m\omega^2 u = i\omega\mu\Omega^{+}\nabla_x s^{+}\left(\frac{L}{2}\right) + i\omega\mu\Omega\ \nabla^{-} s_x^{-}\left(\frac{L}{2}\right) - i\omega\gamma E(\Omega^{+}-\Omega^{-}) \tag{17}$$

It can be seen that in this geometry the liquid crystal can transmit only viscous and electromechanical coupling forces onto the bounding plates. We will see later that this fact causes that the resonance frequencies are

independent of the mass of the bounding plate.

Calculation

To perform calculations the sample is divided into three parts : a, b and c along its thickness.

a; $-\lambda < x < \lambda \quad (\lambda \longrightarrow 0)$ (the centre of the sample)

In the $\lambda \longrightarrow 0$ limit Eq.(14) can be replaced by the set of equations

$$\nabla_x^2(s^+ + s^-) + \frac{i\omega\rho}{\mu}\cdot(s^+ + s^-) = 0 \tag{18a}$$

$$\nabla_x^2(s^+ - s^-) + \frac{i\omega^2\rho - 2i\check{c}}{\omega\mu}\cdot(s^+ - s^-) = \frac{2\gamma E}{\mu\lambda} \quad . \tag{18b}$$

Since $\lambda \longrightarrow 0$ the solution is expected to be constant,

$$\begin{aligned} s^+ + s^- &= 0 \\ s^+ - s^- &= \frac{-i\omega\gamma E}{\omega^2\rho - 2\check{c}} \quad , \end{aligned} \tag{19}$$

i.e. in the middle of the sample the <<< and >>> domains are vibrating with a phase difference of π.

b; $\lambda < x < \frac{L}{2} \quad (\lambda \longrightarrow 0)$ (the upper half of the sample)

Since $\delta(x)=0$ in this interval the equations of motion (see Eq.(14)) read:

$$\nabla_x^2(s^+ + s^-) + \frac{i\omega\rho}{\mu}\cdot(s^+ + s^-) = 0 \tag{20a}$$

$$\nabla_x^2(s^+ - s^-) + \frac{i\omega\rho}{\mu}\cdot(s^+ - s^-) - \frac{2i\check{c}}{\omega\mu}\cdot\frac{s^+ - s^-}{1-\frac{2|x|}{L}} = 0 \tag{20b}$$

which is supplemented by the boundary condition Eq(15) at $x=\frac{L}{2}$ and Eq.(19) at $x=\lambda\longrightarrow 0$.

Equation (20a) has the solution of

$$s^+ + s^- = 2u = 2C_1\cdot\mathrm{ch}(i\sqrt{i}\varkappa) \quad \text{with } \varkappa = \sqrt{\frac{\omega\rho}{\mu}}\cdot\frac{L}{2} \tag{21}$$

In order to find the solution of Eq.(20b) first we will

use the substitutions

$$s^+ - s^- = \left(\frac{2x}{L}-1\right)\cdot e^{-i\sqrt{i}\varkappa\left(\frac{2x}{L}-1\right)}\cdot w(\eta) \tag{22}$$

$$\eta = 2i\sqrt{i}\varkappa\cdot\left(\frac{2x}{L}-1\right) \quad ; \quad a = 1 + \frac{i\sqrt{i}\varkappa\check{c}}{\omega^2\rho}$$

to transform Eq.(20b) into

$$\eta\cdot w''(\eta) + (2 - \eta)\cdot w'(\eta) - a\cdot w(\eta) = 0 \tag{23}$$

which is the confluent hypergeometric differential equation. Its solution is the Kummer function[13]:

$$w(\eta) = C_2\cdot F(a,2,\eta)\ , \tag{24}$$

where the coefficient C_2 is to be determined from the boundary condition Eq.(19). Returning to Eq.(22) we obtain

$$s^+ - s^- = -\frac{\gamma\omega E\cdot\left(\frac{4x}{L}-2\right)}{\lambda(\omega^2\rho-2\check{c})}\cdot\frac{F\left(a,2,i\sqrt{i}\varkappa\left(\frac{4x}{L}-2\right)\right)}{F\left(a,2,-2i\sqrt{i}\varkappa\right)}\cdot e^{-i\sqrt{i}\varkappa\frac{2x}{L}} \tag{25}$$

Substituting Eqs.(21) and (25) into the equation of motion of the upper plate Eq.(17) we can calculate the coefficient C_1. Finally the amplitude of the displacement of the upper plate can be expressed as

$$u = -\frac{\gamma\mu E(\Omega^+ - \Omega^-)}{mL\lambda(\omega^2\rho-2\check{c})}\cdot\frac{\dfrac{4\ e^{-i\sqrt{i}\varkappa}}{F(a,2,-i\sqrt{i}\varkappa)} - \dfrac{iL\lambda(\omega^2\rho-2\check{c})}{m\omega}}{1 + \dfrac{4\sqrt{i}\varkappa\mu(\Omega^+ + \Omega^-)}{Lm\omega}\tanh(i\sqrt{i}\varkappa)} \tag{26}$$

c: $-\frac{L}{2} < x < -\lambda \quad (\lambda \longrightarrow 0)$ (lower half of the sample)

The equations of motion are the same as those in the case of b; except that the sign of x in the denominator of the interaction term in Eq.(20b) must be changed to opposite. However, we are not interested in the solution of them since within the approximation we use it has no influence onto the motion of the upper plate.

CONCLUSIONS

Equation (26) seems rather complicated, however the main characteristics are visible. It is clear that the displacement is proportional to the electric field, the electromechanical coupling constant and the difference of the <<< and >>> domain surfaces, while it is inversely proportional to the mass of the bounding plate and the thickness interval, where the bend of smectic layers takes place.

It is also easy to deduce that the displacement possesses a resonance at a frequency f_r which is determined by the equation $\omega^2\rho - 2\check{c} = 0$. This yields

$$f_r = \frac{1}{2\pi}\cdot\sqrt{\frac{2\check{c}}{\rho}} \qquad (27)$$

i.e. the resonance frequency depends on material parameters but is independent of the mass of the moving plate. Since $\check{c}$ describes the influence of the zig-zag defects, this resonance originates in the chevron structure.

The characteristics mentioned above can be checked by numerical calculation of the spectrum of the absolute value of the displacement $|u|$. We have chosen typical values for the material and sample parameters as listed below:

$\rho=10^{3}\mathrm{kgm}^{-3}$; $\check{c}=10^{11}\mathrm{Nm}^{-4}$; $\mu=10^{-2}\mathrm{Pas}$; $m=10^{-2}\mathrm{kg}$

$\gamma=10^{-12}\mathrm{As}^{2}\mathrm{m}^{-2}$; $E=10^{6}\mathrm{Vm}^{-1}$; $L=2\cdot10^{-5}\mathrm{m}$; $\lambda=10^{-8}\mathrm{m}$

$\Omega^{+}+\Omega^{-}=10^{-3}\mathrm{m}^{2}$; $(\Omega^{+}-\Omega^{-})/(\Omega^{+}+\Omega^{-})=0.1$

The calculated spectrum is shown in Fig.4. Comparing it to the measured spectra[5,6], we can draw the following conclusions.

First, since the resonance at f_r is mass independent, it may correspond to the measured resonances at f_1 and f_2. However, our model yields only one resonance in the spectrum. This may be due to the approximations used in our model, namely that we have taken into account the effect of chevrons in an averaged form.In a real sample there may be

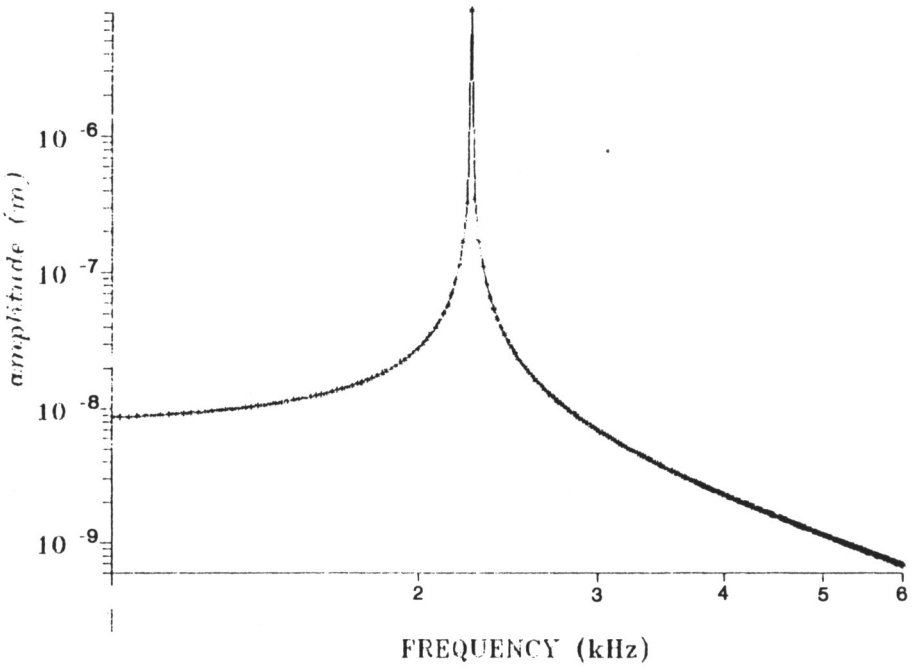

FIGURE 4. Calculated theoretical spectrum of the electromechanical vibration of a typical homogeneous planar S_C^* liquid crystal.

inhomogeneities in the zig-zag defects (various č values at different places) which can result in multiple resonances.

Second, the calculated resonance is sharper than the experimental ones. It may be caused by two facts. In a real material the displacement is limited by the nonlinearities, which are not incorporated in this calculation, while Eq.(26) diverges at f_r. The other cause may be the inhomogeneity mentioned above (i.e. a distribution of č) which can result in wider resonance peaks.

Third, the amplitude is proportional to $\Omega^+ - \Omega^-$ which means that there is no vibration if the domains of two kinds are of equal size. Since the nucleation of <<< and >>> domains is a more or less accidental process, $\Omega^+ - \Omega^-$ may take rather different values. This can give account of the scattering of amplitude data measured on various samples of

the same compound[6].

Furthermore there may be a correlation between $\Omega^+-\Omega^-$ and the average domain size. This latter quantity varies in a wide range depending on the compound, e.g. in FK4 it was in the cm^2 range, while in CS1011 domains of typically $1mm^2$ area were observed[6]. The larger a monodomain the greater $\Omega^+-\Omega^-$ and hence the larger the amplitude of vibration. This conclusion is in agreement with experimental findings[6,9].

Focal conic texture

In the previous sections we discussed homogeneous planar S_C^* samples, now we would like to touch shortly upon focal conic textures.

There is a crucial difference between the two textures in the packing of smectic layers. In the focal conic texture the majority of smectic layers are not parallel to the vibration direction and this holds even at the surfaces of the bounding plates. Though a precise deduction is by far beyond the scope of the present paper we expect that in this case an elstic force is transmitted from the liquid crystal to the substrates too. This means that into the boundary condition Eq.(17) one should introduce a restoring force -ku yielding

$$(m\omega^2-k)u=i\omega\mu\Omega^+\nabla_x s^+\left(\frac{L}{2}\right)+i\omega\mu\Omega\ \nabla^- s_x^-\left(\frac{L}{2}\right)-i\omega\gamma E(\Omega^+-\Omega^-) \qquad (27)$$

where k is an effective "spring constant" characterizing the elastic response of deformed focal conics. This equation describes a resonance at a frequency of

$$f_R = \frac{1}{2\pi}\cdot\sqrt{\frac{k}{m}}$$

which may correspond to measured resonance at f_o since it depends on the mass of the bounding plate. The presence of focal conic defects requires a modification of our model as well, however we think that its main feature – the existence of a mass independent resonance – would be preserved. This means that in focal conic samples the resonances of both type[5,6] can be explained.

SUMMARY

The influence of zig-zag defects on the electromechanical responses of planar S_C^* liquid crystals was considered. The calculation was based on a phenomenological modification of the continuum theory of uniform planar S_C^* samples. This modification has taken into account the influence of zig-zag defects by an effective volume force acting on monodomains. This force is due to the fact that in domains with oppositely bent smectic layers the electromechanical vibration occurs with different phases and so the smectic layers in zig-zag defects must be compressed. According to the geometry of zig-zag defects, in homogeneously aligned planar samples the elastic response of defects is restricted to the interior of the sample, consequently the resonance frequency is not sensitive to the mass of the moving plate. In focal conic textures, however the elastic response extends to the boundaries allowing for another resonances.

Our model has pointed out that the domain size plays a determining role in the electromechanical response of S_C^*. It would be very interesting to find out which factors determine the sizes of domains. On the basis of our experimental findings we guess that the monodomain areas decrease as the spontaneous polarization increases. It would be also very interesting to investigate the influence of the antiparallel SiO oblique evaporation, because it was reported[14] that this type of boundary treatment yields uniform tilted structure. This structure change should modify the frequency spectra. (Probably no resonance is present in this case.)

As a summary we can say, that we could explain the resonances found in several planar S_C^* liquid crystal samples. All main characteristics are explained by a continuum theory taking into account the effect of zig-zag domains and the focal-conic defects. On the basis of this

calculation, we state, that by the analysis of the electromechanical responses, it is possible to determine some material parameters and to deduce certain consequences regarding on the sample structures.

ACKNOWLEDGEMENT

The authors thank Dr. I. Jánossy, T. Kósa, Dr. G. Pór and Dr. Á. Buka for helpful discussions.

REFERENCES

1. N. A. Clark and S. T. Lagerwall, Appl. Phys. Lett., 36, 899 (1980)
2. T. P. Rieker, N. A. Clark, G. S. Smith, D. S. Parmar, E. B. Sirota and C. R. Safinya, Phys. Rev. Lett., 59, 2658 (1987)
3. Y. Ouchi, H. Takezoe and A. Fukuda, Jpn. J. Appl. Phys., 26, 1 (1987)
4. A. Jákli, L.Bata, Á. Buka, N. Éber and I. Jánossy, J. Physique Lett., 46, L-759 (1985)
   A. Jákli, L.Bata, Á. Buka and N. Éber, Ferroelectrics, 69, 153 (1986)
5. G. Pór and Á. Buka, J. Physique, 50, No.7, 783 (1989)
6. A. Jákli and L. Bata, submitted to J. Physique (1989)
7. A. Jákli and L. Bata, submitted to Liquid Crystals (1989)
8. P. Pieranski, E. Guyon and P. Keller, J. Physique, 36, 1005 (1975)
9. A. Jákli and L. Bata, submitted to Mol. Cryst. Liq. Cryst. (1989)
10. A. Fukuda, Y. Ouchi, H. Arai, H. Takano, K. Ishikawa and H. Takezoe, presented in 12th Int. L. C. C. (FE02), to appeare in Liquid Crystals (1989)
11. N. A. Clark, T. P. Rieker and J. E. MacLennan, Ferroelectrics, 85, 79 (1988)
12. N. Éber, L. Bata and A. Jákli, Mol. Cryst. Liq. Cryst., 142, 15 (1987)
13. E. Kamke, Differentialgleichungen Lösungsmethoden und Lösungen I. Gewöhnliche Differentialgleichungen, (Leipzig, 1959)
14. Y. Ouchi, J. Lee, H. Takezoe, A. Fukuda, K. Kondo, T. Kitamura and A. Mukoh, Jpn. J. Appl. Phys., 27, No.11, L1993 (1988)